Check for updates

View Article Online
View Journal

JAAS

Journal of Analytical Atomic Spectrometry

Accepted Manuscript

This article can be cited before page numbers have been issued, to do this please use: Z. Zhou, M. Schmitt, A. Seubert and D. Beauchemin, *J. Anal. At. Spectrom.*, 2026, DOI: 10.1039/D6JA00095A.

This is an Accepted Manuscript, which has been through the Royal Society of Chemistry peer review process and has been accepted for publication.

Accepted Manuscripts are published online shortly after acceptance, before technical editing, formatting and proof reading. Using this free service, authors can make their results available to the community, in citable form, before we publish the edited article. We will replace this Accepted Manuscript with the edited and formatted Advance Article as soon as it is available.

You can find more information about Accepted Manuscripts in the Information for Authors.

Please note that technical editing may introduce minor changes to the text and/or graphics, which may alter content. The journal's standard Terms & Conditions and the Ethical guidelines still apply. In no event shall the Royal Society of Chemistry be held responsible for any errors or omissions in this Accepted Manuscript or any consequences arising from the use of any information it contains.

ROYAL SOCIETY OF CHEMISTRY

rsc.li/jaas

View Article Online
DOI: 10.1039/D6JA00095A

ARTICLE

Optimization of an Infrared-Heated Sample Introduction System for Single-Particle Inductively Coupled Plasma Mass Spectrometry Analysis of Metal-Labelled Ion-Exchange Polymer Microparticles

Received 00th January 20xx,

Accepted 00th January 20xx

DOI: 10.1039/x0xx00000x

Zichao Zhou[a], Matthias Schmitt[b], Andreas Seubert[b], Diane Beauchemin[a]

Single particle inductively coupled plasma mass spectrometry (spICPMS) is increasingly employed for quantification of microplastics (MPs). However, routine analysis of polymer MPs remains constrained by the poor transport efficiency (TE) of conventional pneumatic nebulization systems and by limited sensitivity for carbon-based detection. In this study, an infrared (IR)-heated modified baffled cyclonic spray chamber was used for spICPMS, and an electrostatic Ba^{2+} labeling strategy was introduced to enable sensitive, particle-by-particle characterization of functionalized polymer MPs. For 4.5-µm sulfonated polystyrene/divinylbenzene ion-exchange MPs, IR heating (135–150 °C) increased the number of detected events approximately 20-fold relative to a Scott double-pass chamber, yielding a TE of 60 ± 7%. For 10-µm MPs, 11% TE resulted under optimized conditions, extending the practical upper size range. For unlabeled MPs monitored via $^{13}C^+$, the IR-heated system increased event counts by greater than 20-fold (from 170 ± 40 to 4300 ± 600 for 4.28-µm MPs; from 7.0 ± 4 to 350 ± 50 for 10-µm MPs). Ba^{2+} labeling of sulfonate sites provided accurate size estimates (4.2 ± 2.4 µm and 10.3 ± 3.6 µm) consistent with independent scanning electron microscopy measurements, demonstrating a potential characterization method using functional-group-associated heteroatom content at the single-particle level.

Introduction

Microplastics (MPs) are now detected across marine, freshwater, and terrestrial ecosystems, and are increasingly recognized in the context of human exposure.[1] Their significance extends beyond particle abundance and polymer identity, as plastics may contain metal-based tags, and metalloids may be absorbed from surrounding media.[2,3] As these components can modulate weathering behavior, environmental transport, and toxicological outcomes, MPs analysis requires tools that quantify both MPs and their elemental signatures. In fact, the study of MPs has expanded to include viruses to evaluate their combined effects on environmental and human health.[4]

MPs are recognized as pervasive particulate contaminants in aquatic and terrestrial environments.[3,5] However, meaningful exposure and risk assessments remain constrained by the difficulty of measuring particle number concentration (PNC) and size distributions at environmentally relevant levels, especially in complex matrices. For plastic specifically, inductively coupled plasma mass spectrometry (ICPMS) approaches typically require either microwave digestion or intentional metal tag to enable quantification of the polymer through its elemental composition.[6,7]

Single particle ICPMS (spICPMS) has become an important technique for high-throughput characterization of metal-containing particles. The approach detects individual transient ion signals generated when individual particles are atomized and ionized in the plasma, enabling estimation of particle mass and size if density, shape, and composition are known, alongside dissolved analyte concentration.[8] Compared with ensemble methods, spICPMS provides particle-by-particle information and can rapidly generate particle mass/size distributions, making it useful for screening particles in products and environmental extracts.[9]

Several studies have described the detection of micrometer-sized particles by monitoring C isotopes, despite the low degree of ionization of C in the ICP and the variety of potential non-particulate carbon sources.[8,10–13] Figures of merit have been improved by using ICP tandem mass spectrometry.[11] However, the low sensitivity and the elevated background signal remain critical limitations of this approach.[14,15] Recently, ICP time-of-flight(TOF) MS was used for the quasi-simultaneous detection of $^{12}C^+$ and doped rare earth elements in MP beads.[16]

At the same time, the heteroatom content of various polymer particle types can be exploited for detection using spICPMS, providing chemical information that aids particle identification. Such a heteroatom-based approach was employed for monitoring polytetrafluoroethylene (PTFE) particles through detection of the $^{138}Ba^{19}F^+$ polyatomic ion formed upon addition of barium nitrate to the carrier solution.[17]

[a] Queen's University, Department of Chemistry, 90 Bader Lane, Kingston, ON K7L 3N6, Canada.
[b] University of Marburg, Faculty of Chemistry, Hans-Meerwein-Str. 4, 35043 Marburg, Germany

Electronic Supplementary Information (ESI) available: Tables S1 and S2, and Figures S1-S4. See DOI: 10.1039/x0xx00000x

Open Access Article. Published on 06 May 2026. Downloaded on 5/7/2026 1:53:13 AM.
This article is licensed under a Creative Commons Attribution-NonCommercial 3.0 Unported Licence.

Journal of Analytical Atomic Spectrometry Accepted Manuscript

View Article Online
DOI: 10.1039/D6JA00054

Open Access Article. Published on 06 May 2026. Downloaded on 5/7/2026 1:53:13 AM.
This article is licensed under a Creative Commons Attribution-NonCommercial 3.0 Unported Licence.

When plastics are metal-tagged, the same spICPMS principle can be extended to nanoplastics or MP fragments by treating the metal label as the measurable "reporter," enabling quantification of particle number and size distribution through the tracer mass.[7] A complementary approach to the direct determination of C or covalently attached heteroatoms is the labeling of particles with abundant isotopes that are not susceptible to common ICPMS interferences, which increase sensitivity. Tagging carboxylated nanoplastics with positively charged gold nanoparticles (NPs) was found to be the most effective approach, while direct Ag^+ metal labeling was insufficient for sensitive detection.[18,19] Additionally, an optimized tagging with NPs was developed to label common plastic types and detect them in the presence of matrix NPs.[20]

Despite these advances, conventional spICPMS calibrated with dissolved standards requires independent measurements of sample uptake rate and sample transport efficiency (TE) to convert signal intensity into particle mass, which adds labor and introduces error sources.[21,22] In addition, standard pneumatic nebulization is inherently inefficient, with TE below 1% for MPs and cells using a sample introduction system consisting of a pneumatic nebulizer fitted into a Scott double-pass spray chamber.[23] As a result, only a small fraction of particles reaches the plasma, which increases sample consumption and reduces the number of detectable particle events.These limitations are especially problematic where sample volume may be limited, target MPs may be rare, and matrices can elevate background signals.[24] Although using a linear pass spray chamber designed for the analysis of cells improved TE, a degradation of TE resulted when the size of the cell increased from 2-3 µm to 6 µm.[25–27]

The upper size limit in spICPMS is also limited by the sample introduction system. Aerosol droplets produced by pneumatic nebulization, following passage through the spray chamber, are generally less than 8 µm in diameter, and the sample transport rate must remain sufficiently low to avoid plasma extinction.[28] Falling-tube devices and vertically downward-pointing ICP-TOFMS configurations have been employed to extend the upper size limit to approximately 20 µm.[14]

One infrared (IR) heated sample introduction system provides total consumption for NPs.[29,30] As heating the aerosol reduces the droplet size and noise originating from the desolvation and vaporization of droplets in the ICP,[31,32] it may allow larger MPs to reach the plasma. The aim of this proof-of-concept study was to expand the set of methodologies for the analysis of MPs by assessing the performance of an IR-heated sample introduction system and an electrostatic metal labeling procedure.[11,18,33] No IR-heated sample introduction system has previously been used for the measurement of MPs. Also for the first time, size characterization of functionalized MPs was based on electrostatic metal ion labeling of functional groups, with the aim to increase sensitivity.[34]

Optimization of the IR-heating temperature and the sample uptake rate was performed using Ba-labeled sulfonated polystyrene (PS)/divinylbenzene (DVB) MPs to obtain a stable, high-contrast MP signal for TE evaluation. The use of an alkaline earth metal cation for labelling should significantly improve binding selectivity and therefore reduce the background. Furthermore, the resulting stoichiometric labelling allows counting of the functional groups based on the Ba atoms. The optimized IR-heated sample introduction system was then applied to size characterization of unlabeled MPs detected via ^{13}C and labelled MPs detected via ^{138}Ba and S content. A protocol for introducing these highly hydrophobic materials is also presented.

Experimental

Instruments

A Varian 820MS ICP-MS instrument (Mulgrave, Australia) or a NexION 2000 ICPMS instrument (PerkinElmer, Waltham, MA, USA) equipped with Syngistix nanosoftware was employed without any collision or reaction gas to maximize sensitivity. For optimization, solutions and suspensions of MPs were introduced at 25 to 300 µL min^{-1} using a standalone peristatic pump. The sample uptake rate was determined daily and obtained from 5-min aspiration of water in triplicates.

The sample introduction system consisted of a 25-mL modified baffled cyclonic spray chamber featuring a 2-mm gap between the top of the modified baffle and the upper surface of the spray chamber, a shortened neck, and an L-shaped elbow connection (JRV Scientific Glass, Montreal, QC, Canada),[29,30] and an SC175 single-cell nebulizer (Burgener Research Inc., Mississauga, ON, Canada) designed for low-flow operation and introduction of larger particles. A ceramic rod IR heater (Elstein-Werk, Northeim, Germany) inserted into the modified baffle, and a ceramic beaded rope IR heater (Normangee, TX, USA) wrapped around the elbow connection and the base of the torch heated the system. Two thermocouples positioned next to the pen heater and underneath the rope heater were connected to separate DigiTrol II temperature controllers (GLAS-COL Apparatus Company, Terre Haute, IN, USA). The entire assembly was insulated with glass-fiber heat resistant tape and aluminum foil to minimize heat loss and maintain thermal stability.

For comparison, both ICPMS instruments were also operated with the SC175 single-cell nebulizer inserted in their standard spray chamber: a Scott double-pass spray chamber (SCP Science, Baie d'Urfé, QC, Canada) in Peltier cooling system on the Varian 820MS and a baffled cyclonic C3 high-sensitivity glass cyclonic spray chamber with a matrix gas port (PerkinElmer) on the NexION 2000B. The operating conditions used with the standard and IR-heated sample introduction systems on the two instruments are summarized in Table 1.

Chemicals

External calibration solutions for C determination were freshly prepared from tartaric acid in glassware to minimize C contamination.[10] Ba standard solutions (0.1–100 ng L^{-1}) were prepared in 2% v/v HNO_3 from 10000 mg L^{-1} Ba solutions (SCP Science), sub-boiled HNO_3 (ACS grade; Fisher Scientific, Ottawa, ON, Canada) purified in a sub-boiling distillation system (Savillex, Minnetonka, MN, USA) and doubly deionized water (DDW) (18.2 MΩ

This journal is © The Royal Society of Chemistry 2026

Please do not adjust margins

Journal of Analytical Atomic Spectrometry Accepted Manuscript

JAAS ARTICLE

View Article Online
DOI: 10.1039/D6JA00095A

Table 1. ICPMS operating conditions

	Varian 820MS		NexION 2000B	
Spray chamber	Scott double pass	IR-heated modified cyclonic	Baffled cyclonic	IR-heated modified cyclonic
Ar plasma gas flow rate (L min^{-1})	18	18	15	15
Ar auxiliary gas flow rate (L min^{-1})	1.8	1.8	1.2	1.2
RF power (kW)	1.3	1.3	1.6	1.6
Ar nebulizer gas flow rate (L min^{-1})	0.98	0.98	1.0	1.0
Dwell time (µs)	10000	10000	50	50
Operating temperature (°C)	3	150 °C	20	150
Sample uptake rate (µL min^{-1})	333	75	75	75
Monitored signal	$^{13}C^+$, or $^{138}Ba^+$			

cm) (Arium Pro UV/DI System, Sartorius Stedim Biotech, Goettingen, Germany). The performance of the standard sample introduction system on the Varian 820MS and NexION 2000B was optimized using a 5 µg L^{-1} multielement tuning solution.

Labeling of MPs

PS/DVB MPs were prepared and characterized as described previously (Table S1).[34,35] Two resins were selected as model materials. Particles of type A offer a high degree of sulfonation and narrow homogeneous size distribution, with an average diameter of 4.45 µm. Type B particles have a lower degree of sulfonation and a broad and heterogeneous size distribution around an average of 10.0 µm.

Briefly, a suspension of 5 mg dried polymer MPs, 0.5 mL ethanol, 0.5 mL water and 0.1 mL saturated $Ba(NO_3)$ labeling solution was homogenized and incubated overnight at 21 °C. The MPs were extracted seven times with 20/80% (v/v) (ethanol/water) and then with water to remove unbound metal ions. The labeled MPs were dried overnight at 60 °C and were weighed to determine the mass concentration of the respective slurry. A stock suspension of 5000 mg L^{-1} was prepared in 1 mM Triton X-100, which was stored at room temperature and was stable for over 6 months.[34] Prior to analysis, the stock suspension was sonicated and diluted to 10 mg L^{-1} with 1 mM Triton X-100 (or DDW for unlabeled MPs). Diluted slurries of MPs were sonicated for30 min before analysis and then sonicated for 10 min at 30-min intervals throughout the analysis to minimize aggregation.

Transport efficiency and particle number concentration

Under the conditions in Table 1, the ratio of detected MP events over the total number of MPs delivered to the sample introduction system during the measurement period corresponded to TE. The particle frequency method was selected over the particle mass approach[21] because type A and type B MPs are not certified in mass whereas their PNC could be measured to determine the total number of MPs delivered to the nebulizer during the measurement period. The PNC of MPs suspension was determined using a Neumann counting chamber (Marienfeld, Lauda, Germany) with two replicate fillings per sample combined with optical microscopy. Twenty images at 10x magnification were taken per replicate using a Axiotech 100HD microscope (Zeiss, Jena, Germany) equipped with a Canon EOS 1200D (Canon, Tokio, Japan) camera. Images were processed using the ImageJ2 software with Fiji package to determine PNCs (included in Table S1).

Optimization

A multivariate optimization of the sample uptake rate in the 25-75 µL min^{-1} range and IR-heating temperature in the 20-250 °C range was performed using a 1 mg L^{-1} suspension of 4.28 µm labeled MPs. A central composite design was generated with Minitab 18 (State College, Pennsylvania, USA) statistical software (Table S2). The optimization was performed on the Varian 820MS whereas evaluation of the performance of the optimized IR-heated sample introduction system was carried out on the NexION 2000B.

Data processing

The data collected in time-resolved mode were exported and processed using Excel (Microsoft, Redmond, WA, USA). The same statistical model was applied for particle identification whether unlabeled MPs were monitored using $^{13}C^+$ or labeled MPs were monitored using $^{138}Ba^+$. A threshold of three times the standard deviation of the average signal was used to discriminate between MP events and the background. The procedure was iterated to account for all MP events independently of the number of detected events. External calibration with standard solutions of C (tartaric acid) and Ba was used to convert MP signal into MP mass for unlabeled and Ba-labeled MPs respectively. Solution concentration was converted into mass flux by multiplying it by the dwell time, sample uptake rate and TE. The IR-heated sample introduction system provided 100% TE for standard solutions.[30] For the conventional sample introduction system, the solution TE was measured using a certified Au NPs suspension. The acquired data were further processed using Excel 365 (Microsoft) and GraphPad Prism 9 (GraphPad Software 225, Boston, MA, USA). Varian 820MS data were corrected for the average quadrupole settling time of 41 ms per dwell time period when monitoring a single m/z ratio, as described previously.[36] Also, TE was corrected by multiplying it by the fraction of total acquisition time during which data were actually collected.[37,38]

Results and discussion

Effect of temperature and sample uptake rate on TE

Open Access Article. Published on 06 May 2026. Downloaded on 5/7/2026 1:53:13 AM.
This article is licensed under a Creative Commons Attribution-NonCommercial 3.0 Unported Licence.

Journal of Analytical Atomic Spectrometry Accepted Manuscript

Please do not adjust margins

View Article Online
DOI: 10.1039/D6JA00095A

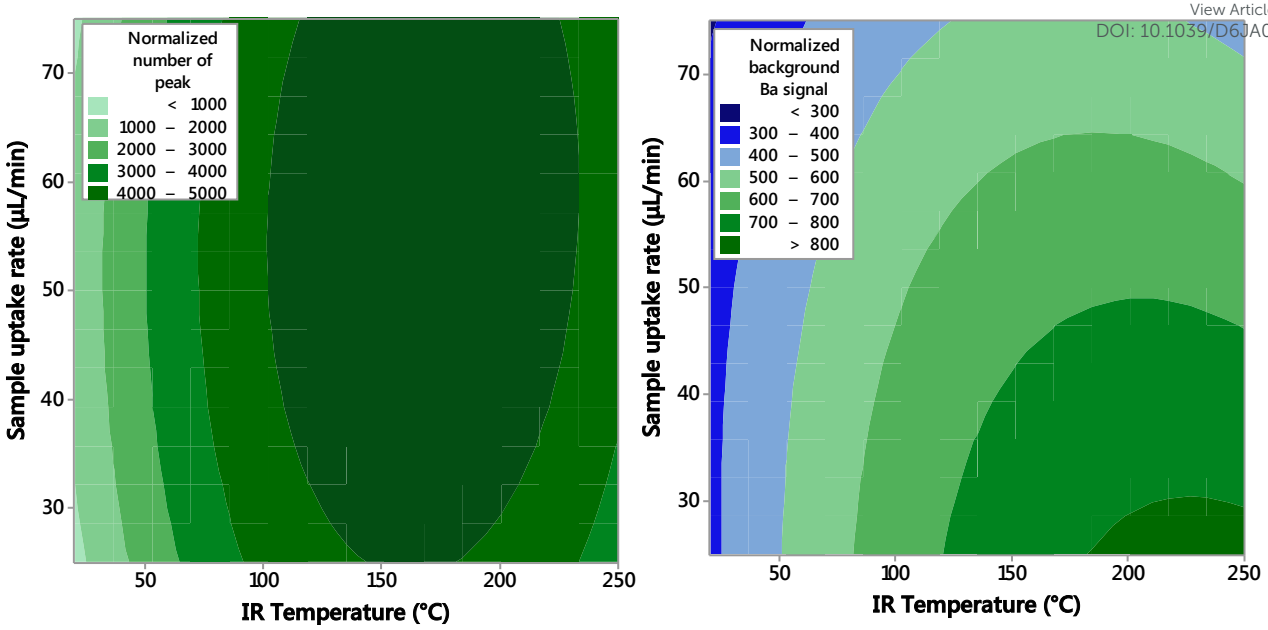

Fig. 1 Contour plot of normalized particle number for Ba^{2+}-labelled resin of type A (1 mg L^{-1}) *versus* sample uptake rate and IR-heating temperature (**left**). Contour plot of blank-subtracted MPs signal for Ba^{2+}-labelled resin of type A *versus* sample uptake rate and IR-heating temperature (**right**).

Using 4.5 µm Ba-labeled sulfonated PS/DVB MPs of type A to provide a stable, high-contrast MP signal for TE evaluation, IR-heating temperature and sample uptake rate were optimized while monitoring the number of detected peaks, which reflects TE, and the background signal level, which influences the theoretical method detection limit (Fig. 1). The maximum number of detected peaks was observed in the temperature range of 135–220 °C, and this maximum was not very dependent on sample uptake rate, as confirmed by the Pareto chart (Fig. S2). However, as temperature increased and sample uptake rate decreased, background signal intensity increased, indicating that some Ba-labeled MPs lost their Ba^{2+} tags into the surrounding solution. Thus, an upper temperature threshold may exist for introduction of electrostatically tagged MPs, beyond which tag stability becomes compromised.

An IR-heating temperature of 150 °C at 75 µL min^{-1} sample uptake rate (Table 1) provided the best compromise in terms of maximizing MPs number while also minimizing background Ba signal. Compared to 508 ± 57 MPs detected using a Scott double-pass spray chamber at 3 °C and 333 µL min^{-1}, the number of detected MPs increased 10-fold with the IR-heated system for the same suspension despite the sample uptake rate being only 75 µL min^{-1}. The higher sample uptake rate with the Scott double-pass spray chamber was required to detect enough MP events. Based on the calculated PNC, this corresponds to a TE of 60 ± 7% with the IR-heated system. Although this represents a substantial improvement, further optimization will be required to achieve total consumption.

Size characterization of unlabeled MPs

The performance of the optimized IR-heated sample introduction system was also evaluated for unlabeled MPs on a NexION 2000B instrument, which has negligible settling time (in contrast to the Varian 820 MS instrument that takes on average 41 ms per dwell time period to send data to the computer, during which no data acquisition can occur). Type A (4.28 µm) and type B (10 µm) MPs

Table 2. Characterization of type A (4.5 µm) and type B (10 µm) MPs using two sample introduction systems on the NexION 2000

	Standard cyclonic spray chamber	IR-heated sample introduction system
Average $^{13}C^+$peak intensity of type A MPs (counts)	12.3 ± 3.2	10.2 ± 2.1
Average size of type A MPs (µm)	5.6 ± 1.7	4.8 ± 1.4
Average $^{13}C^+$peak intensity of type B MPs (counts)	67.8 ± 6.0	98.4 ± 5.3
Average size of type B MPs (µm)	7.6 ± 1.0	9.2 ± 2.1
Average % TE of type A MPs (n=3)	2.13 ± 0.50	53.8 ± 7.5
Average % TE of type B MPs (n=3)	0.23 ± 0.13	11.7 ± 1.6
Method detection limit (µm)[1]	1.8	1.7

1. Calculated based on ^{13}C background signal left after removing the MPs signal and assuming spherical geometry

Open Access Article. Published on 06 May 2026. Downloaded on 5/7/2026 1:53:13 AM.
This article is licensed under a Creative Commons Attribution-NonCommercial 3.0 Unported Licence.

Journal of Analytical Atomic Spectrometry Accepted Manuscript

 This journal is © The Royal Society of Chemistry 2026

Please do not adjust margins

View Article Online
DOI: 10.1039/D6JA00095A

Open Access Article. Published on 06 May 2026. Downloaded on 5/7/2026 1:53:13 AM.
This article is licensed under a Creative Commons Attribution-NonCommercial 3.0 Unported Licence.

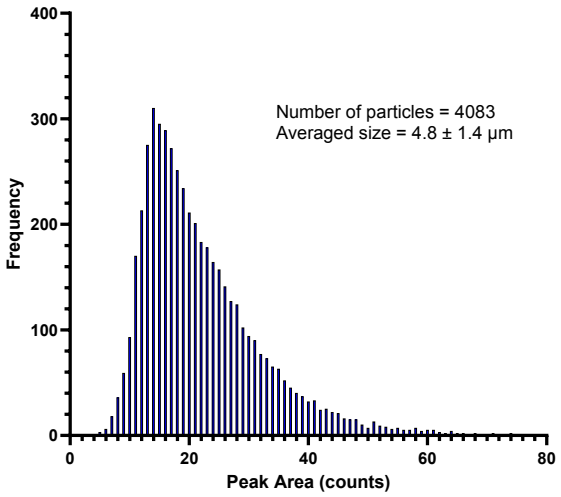

Fig. 2 Peak area distribution of the 4.5 µm type A MPs obtained using the optimized IR-heated sample introduction system

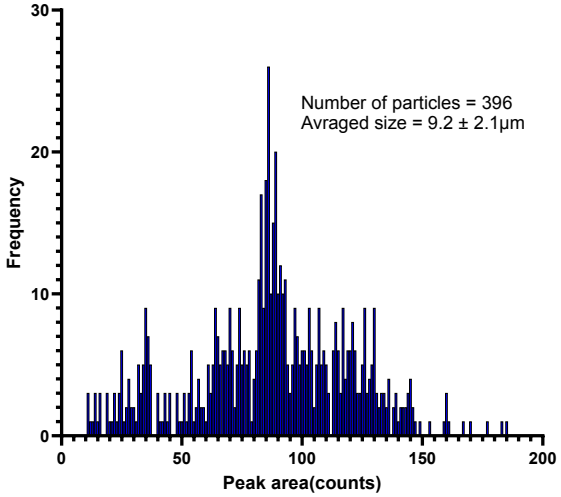

Fig. 3 Peak area distribution of the 10 µm type B MPs obtained using the optimized IR-heated sample introduction system

were analyzed while monitoring $^{13}C^{+}$ (Table 2). For the 4.28 µm MPs, the number of detected peaks increased from 188 to 4083 when introducing suspensions of equivalent PNC, representing more than 20-fold improvement (Fig. S3 and Fig. 2) versus that achieved with a standard baffled cyclonic spray chamber at the same sample uptake rate of 75 µL min^{-1}. This improvement was reflected in TE, which increased from less than 2.1% with the standard system to approximately 55% with IR-heated sample introduction. This TE agrees with the 60 ± 7% obtained when the same IR-heated system was used on the Varian 820MS instrument, indicating that it provides consistent results across ICPMS instruments.

Analysis of 10 µm MPs proved particularly challenging for the standard pneumatic sample introduction system. Being designed to filter out droplets larger than approximately 8 µm, when 3000 MPs were introduced, only 7 MP events were detected. Furthermore, the MP sizes calculated from the ^{13}C calibration were significantly smaller than the known size, indicating that only a subpopulation of smaller

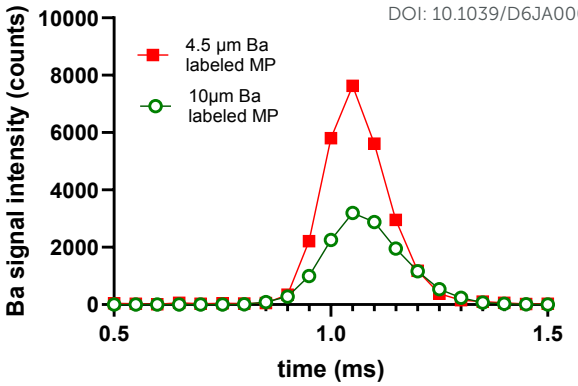

Fig. 4 ^{138}Ba signal obtained at 50 µs dwell time for Ba-labelled individual MPs of type A (4.5 µm) and type B (10 µm).

MPs was successfully transported to the plasma, resulting in an unrepresentative size distribution (Fig. S4).

In contrast, the IR-heated sample introduction system enabled detection of more MP events, yielding a size distribution in agreement with the known size (Fig. 3). This is a result of pre-evaporation of droplets by IR heating, which allows more MPs to reach the plasma, and of the modified spray chamber design, where the baffle gap at the top of the chamber rather than at the base allows larger droplets to flow out of the spray chamber. Hence, the IR-heated sample introduction system improves the TE and enables the measurement of larger MPs while retaining the beneficial features of a cyclonic spray chamber design, such as reduced memory effects, without jeopardizing the detection limit (Table 2).

Size characterization of Ba-labeled microplastics

The PS/DVB ion-exchange MPs employed in this study possess sulfonic acid functional groups as cation-exchange sites (Table S1), which each contain one S atom; consequently, the bulk S mass fraction is directly proportional to the unit mass of each polymer MP. Upon incubation with $Ba(NO_3)_2$, Ba^{2+} ions bind electrostatically to the negatively charged sulfonate sites via cation exchange, resulting in a fixed Ba/S stoichiometry. Ba was selected as the labeling element because it exhibits a high signal-to-noise ratio. The quantity of specifically bound Ba^{2+} is governed by the number of available sulfonate sites. Given that the number of sulfonate sites is proportional to S content, the mass of Ba per MP is thus proportional to the mass of S per MP. This relationship enables estimation of MP mass from the measured Ba signal, assuming a constant degree of sulfonation, which may mostly be only valid for the single batch of MPs used in this work.

When two MPs populations differing in size and sulfonate content were introduced into spICPMS, the duration of the ion cloud was comparable regardless of MP size (Fig. 4). However, for the model MPs, smaller MPs (type A) exhibited a higher Ba signal intensity because of their greater S mass percentage. These particles were reported to be fully porous and the functionalization for the 4 µm particles was shown to be homogeneous throughout global particles surface and bulk.[39] As a linear relationship was previously

Journal of Analytical Atomic Spectrometry Accepted Manuscript

Please do not adjust margins

View Article Online
DOI: 10.1039/D5JA00354A

Open Access Article. Published on 06 May 2026. Downloaded on 5/7/2026 1:53:13 AM.
This article is licensed under a Creative Commons Attribution-NonCommercial 3.0 Unported Licence.

Table 3. Size (µm) of MPs obtained by different methods

MP type	SEM[34]	IR-heated sample introduction system	
		^{13}C	^{138}Ba
A	4.5 ± 0.2	4.8 ± 1.4	4.2 ± 2.4
B	10.0 ± 1.4	9.2 ± 2.1	10.3 ± 3.6

reported between the Ba content by spICPMS and the bulk S percentage for different labelled MPs,[34] the S mass was calculated from the measured Ba mass per particle and the known stoichiometry of Ba^{2+} binding to sulfonate groups (the S/Ba atom ratio being 2.1 ± 0.2, obtained by dividing the S/Ba mass ratio by the S/Ba atomic mass ratio). Using the known S mass percentage, the total MP mass was then calculated and converted to MP diameter assuming spherical geometry and a corrected density based on the composition. Table 3 shows that, compared with scanning electron microscopy (SEM) measurements, spICPMS with the IR-heated sample introduction system provided accurate size determinations. As Ba exhibits a higher signal-to-noise ratio than ^{13}C, such indirect method may yield better detection limit than measuring ^{13}C. Table 4 shows that the improvement in size detection limit depends on the S content of MPs. With MPs containing a relatively small amount of S, the size detection limit is similar using ^{13}C or Ba when using the IR-heated sample introduction system. In contrast, Ba labeling is clearly advantageous for MPs with a relatively high S content. Even the size detection limit with the standard system improves, albeit not as much as with IR heating. The Ba-labeling approach may also enable indirect determination of S mass percentage in MPs on a particle-by-particle basis.

Conclusions and future work

This work demonstrates that IR-heating a modified baffled cyclonic spray chamber can improve the introduction of polymer MPs for spICPMS analysis. Under optimized conditions, TE increased to approximately 55% for 4.5 µm particles and decreased to approximately 11% for 10 µm particles, outperforming standard spray chambers that preferentially exclude larger droplets and MPs, thereby biasing measured size distributions. For direct MP detection using $^{13}C^+$, the IR-heated configuration increased the number of measurable particle events by more than an order of magnitude and enabled representative measurement of 10 µm particles that were largely lost through a conventional cyclonic spray chamber. The higher TE and the capability to analyze larger MPs without sacrificing the operational benefits of cyclonic designs, combined with a similar size detection limit, are practical analytical advantages of the IR-heated sample introduction system. This system will facilitate the detection of microbeads that are widely used in personal care products and end up in the environment.[40]

In parallel, a Ba^{2+} ion-exchange labeling strategy provides a sensitive linked reporter for sulfonated PS/DVB MPs, enabling MP size characterization based on the Ba signal and known sulfur content. Agreement between Ba-derived sizes, SEM and known diameters indicates that metal-ion labeling and IR-heated sample introduction provide accurate MP sizing. Using Ba labeling may also significantly improve the size detection limit compared to $^{13}C^+$ measurement when MPs contain a relatively high amount of S. Ba labeling might be used to indirectly assess functional group inter-particle heterogeneity, which is difficult via direct S detection by quadrupole spICPMS. The approach should facilitate the detection of polyethersulfone MPs that are used in energy, environmental and biomedical applications.[41]

Future work will focus on the measurement of MPs of a wider size range to determine the upper particle size detection limit of the method. Additionally, a multivariate optimization including nebulizer gas flow rate and torch position should be carried out to hopefully achieve 100% TE for MPs, including with larger MPs. Polydisperse MPs samples will also be investigated to assess the performance of the system under compositionally complex conditions for environmental applications. To improve the detection of larger MPs, the design of the modified baffled spray chamber, in particular the gap between the top of the baffle and the top service of the spray chamber, will also be revisited.

Data availability

Data for this article, including optimization and spICPMS measurements are available at Open Science Framework at **https://doi.org/10.17605/OSF.IO/6CW25**

Author Contributions

Zichao Zhou: conceptualization, data acquiring, methodology, writing – original draft, Matthias Schmitt: investigation, formal analysis, data acquisition, methodology, writing – review & editing, Andreas Seubert: conceptualization, methodology, resources, project administration, supervision, writing – review & editing, Diane Beauchemin: funding acquisition, supervision, writing – original draft.

Conflicts of interest

There are no conflicts to declare.

Table 4. Size (µm) detection limit for MPs having different S contents using standard and IR-heated sample introduction systems

Material	% (m/m) S	Standard cyclonic spray chamber		IR-heated system	
		^{13}C	^{138}Ba	^{13}C	^{138}Ba
4-µm type A MPs	7.212	1.8	1.3	1.7	0.7
10-µm type B MPs	0.31 ± 0.03	1.8	3.8	1.7	1.5

This journal is © The Royal Society of Chemistry 2026

Please do not adjust margins

Journal of Analytical Atomic Spectrometry Accepted Manuscript

View Article Online
DOI: 10.1039/D6JA00095A

Acknowledgements

ZZ and DB acknowledge funding from Mitacs (grant IT33380 supported by Burgener Research Inc.) and the Natural Sciences and Engineering Research Council of Canada (grant ALLRP 578516-22). ZZ also thanks Mirah and John Burgener for helpful discussions.

References

1 J. Gigault, H. El Hadri, B. Nguyen, B. Grassl, L. Rowenczyk, N. Tufenkji, S. Feng and M. Wiesner, *Nat. Nanotechnol.*, 2021, **16**, 501–507.

2 T. Kim, S. Eo, W. J. Shim and M. Kim, *J. Hazardous Mat.*, 2025, **498**, 139790.

3 C. Campanale, I. Savino, C. Massarelli and V. F. Uricchio, *NanoImpact*, 2022, **28**, 100438.

4 V. C. Shruti, G. Kutralam-Muniasamy and F. Pérez-Guevara, *Sci. Total Environ.*, 2024, **955**, 177010.

5 S. Harycki and A. Gundlach-Graham, *Anal. Chem.*, 2023, **95**, 15318–15324.

6 J. S. F. Pereira, C. L. Knorr, L. S. F. Pereira, D. P. Moraes, J. N. G. Paniz, E. M. M. Flores and G. Knapp, *J. Anal. At. Spectrom.*, 2011, **26**, 1849–1857.

7 C. Smith, S. Brown, N. Malone and S. Bevers, *Environ. Sci Nano*.

8 E. Bolea-Fernandez, A. Rua-Ibarz, M. Velimirovic, K. Tirez and F. Vanhaecke, *J. Anal. At. Spectrom.*, 2020, **35**, 455–460.

9 F. Laborda, E. Bolea and J. Jiménez-Lamana, *Anal. Chem.*, 2014, **86**, 2270–2278.

10 F. Laborda, C. Trujillo and R. Lobinski, *Talanta*, 2021, **221**, 121486.

11 Z. Liu, Y. Zhu, S. Lv, Y. Shi, S. Dong, D. Yan, X. Zhu, R. Peng, A. A. Keller and Y. Huang, *Environ. Sci. Technol. Lett.*, 2022, **9**, 50–56.

12 C. Trujillo, J. Pérez-Arantegui, R. Lobinski and F. Laborda, *Nanomaterials*, 2023, **13**, 1582.

13 L. Hildebrandt, M. Von Der Au, T. Zimmermann, A. Reese, J. Ludwig and D. Pröfrock, *PLoS ONE*, 2020, **15**, e0236120.

14 F. Sandro, H. Bodo and G. Detlef, *J. Anal. At. Spectrom.*, 2025, **40**, 276–285.

15 M. Resano, M. Aramendía, E. García-Ruiz, A. Bazo, E. Bolea-Fernandez and F. Vanhaecke, *Chem. Sci.*, 2022, **13**, 4436–4473.

16 S. Harycki and A. Gundlach-Graham, *J. Anal. At. Spectrom.*, 2023, **38**, 111–120.

17 F. Gelman, M. Muszyńska, J. Karasiński, O. Lev and L. Halicz, *J. Anal. At. Spectrom.*, 2022, **37**, 2282–2285.

18 J. Jiménez-Lamana, L. Marigliano, J. Allouche, B. Grassl, J. Szpunar and S. Reynaud, *Anal. Chem.*, 2020, **92**, 11664–11672.

19 L. Marigliano, B. Grassl, J. Szpunar, S. Reynaud and J. Jiménez-Lamana, *Molecules*, DOI:10.3390/molecules26237093.

20 Y. Lai, L. Dong, Q. Li, P. Li, Z. Hao, S. Yu and J. Liu, *Environ. Sci. Technol.*, 2021, **55**, 4783–4791.

21 H. E. Pace, N. J. Rogers, C. Jarolimek, V. A. Coleman, C. P. Higgins and J. F. Ranville, *Anal. Chem.*, 2011, **83**, 9361–9369.

22 H. E. Pace, N. J. Rogers, C. Jarolimek, V. A. Coleman, E. P. Gray, C. P. Higgins and J. F. Ranville, *Environ. Sci. Technol.*, 2012, **46**, 12272–12280.

23 P. Goodall, M. E. Foulkes and L. Ebdon, *Spectrochim. Acta Part B .*, 1993, **48**, 1563–1577.

24 S. Lee, X. Bi, R. B. Reed, J. F. Ranville, P. Herckes and P. Westerhoff, *Environ. Sci. Technol.*, 2014, **48**, 10291–10300.

25 S. Miyashita, A. S. Groombridge, S. Fujii, A. Minoda, A. Takatsu, A. Hioki, K. Chiba and K. Inagaki, *J. Anal. At. Spectrom.*, 2014, **29**, 1598–1606.

26 Tsutomu. Nomizu, Satoshi. Kaneco, Tomokazu. Tanaka, Daisuke. Ito, Hiroshi. Kawaguchi and B. T. Vallee, *Anal. Chem.*, 1994, **66**, 3000–3004.

27 R. C. Merrifield, C. Stephan and J. R. Lead, *Environ. Sci. Technol.*, 2018, **52**, 2271–2277.

28 John Burgener and Y. Makonnenb, in *Sample Introduction Systems in ICPMS and ICPOES*, Elsevier, 2020, pp. 57–142.

29 Z. Zhou, A. Al Hejami, M. J. Burgener, J. Burgener and D. Beauchemin, *J. Anal. At. Spectrom.*, 2022, **37**, 1450–1454.

30 Z. Zhou, M. J. Burgener, J. Burgener and D. Beauchemin, *J. Anal. At. Spectrom.*, 2024, **39**, 2078–2086.

31 J. W. Olesik and J. C. Fister, *Spectrochim. Acta Part B*, 1991, **46**, 851–868.

32 A. A. Hejami, M. J. Burgener, J. Burgener and D. Beauchemin, *J. Anal. At. Spectrom.*, 2020, **35**, 1125–1130.

33 A. Bianco, F. Sordello, M. Ehn, D. Vione and M. Passananti, *Sci. Tot. Environ.*, 2020, **742**, 140413.

34 M. Schmitt, *PhD thesis,* Marburg University, 2024.

35 M. Schmitt, M. Egorycheva and A. Seubert, *J. Chromatogr. A*, 2022, **1664**, 462790.

36 R. P. Lamsal, G. Jerkiewicz and D. Beauchemin, *Microchem. J.*, 2018, **137**, 485–489.

37 R. P. Lamsal, G. Jerkiewicz and D. Beauchemin, *Anal. Chem.*, 2018, **90**, 13842–13847.

38 A. Williams, A. Al Hejami and D. Beauchemin, *J. Anal. At. Spectrom.*, 2020, **35**, 2165–2170.

39 M. Schmitt, M. Egorycheva and A. Seubert, *J. Chromatogr. A*, 2023, **1695**, 463934.

40 A. Singh and B.K. Mishra, *J. Cleaner Production*, 2023, **427**, 139082.

41 S. Samitsu, *Polymer*, 2022, **248**, 124744.

Open Access Article. Published on 06 May 2026. Downloaded on 5/7/2026 1:53:13 AM.
This article is licensed under a Creative Commons Attribution-NonCommercial 3.0 Unported Licence.

Journal of Analytical Atomic Spectrometry Accepted Manuscript

Please do not adjust margins

View Article Online
DOI: 10.1039/D6JA00095A

Data for this article, including optimization and spICPMS measurements are available at Open Science Framework at https://doi.org/10.17605/OSF.IO/6CW25

Open Access Article. Published on 06 May 2026. Downloaded on 5/7/2026 1:53:13 AM.
This article is licensed under a Creative Commons Attribution-NonCommercial 3.0 Unported Licence.

Journal of Analytical Atomic Spectrometry Accepted Manuscript